CONF-9210107--23

INTERIM FATIGUE DESIGN CURVES FOR CARBON, LOW-ALLOY, AND AUSTENITIC STAINLESS STEELS IN LWR ENVIRONMENTS*

S. Majumdar, O. K. Chopra, and W. J. Shack
Materials and Components Technology Division
Argonne National Laboratory
Argonne, IL 60439

ANL/MCT/CP--78588

DE93 009202

January 1993

DISCLAIMER

To be published in the Proceedings of the 20th Water Reactor Safety Information Meeting, Oct. 21-23, 1992, Bethesda, MD

*Work supported by Office of Nuclear Regulatory Research, U.S. Nuclear Regulatory Commission FIN Nos. A22122 and A22562. Program Manager Dr. J. Muscara.

Interim Fatigue Design Curves for Carbon, Low-Alloy, and Austenitic Stainless Steels in LWR Environments*

S. Majumdar, O. K. Chopra, and W. J. Shack
Materials and Components Technology Division
Argonne National Laboratory
Argonne, Illinois

Overview of Existing Data

The existing data in the literature on the fatigue of carbon steel in LWR environments have been reviewed to provide a basis for the development of fatigue design curves that account for the effect of LWR environments. The primary published sources of these data are the work by Higuchi and Iida,[1] the data obtained in a test loop at the Dresden 1 reactor by GE[2,3], tests performed by GE/EPRI,[4] and the work by Terrell.[5] In addition, a series of tests has been conducted by B&W in water chemistries characteristic of fossil secondary systems.[6] Although these water chemistries are much different from the LWR chemistries of interest, the temperature and oxygen levels — which appear to be the critical environmental variables — are in the ranges of interest.

A number of trends are clear from the available data. Both temperature and oxygen affect fatigue life. At the very low dissolved-oxygen levels characteristic of PWRs and BWRs with hydrogen water chemistry, environmental effects on fatigue life are modest at all temperatures and strain rates. Increases in dissolved oxygen above ≈0.1 ppm, produce significant reductions in fatigue life. The effect of the dissolved-oxygen increases rapidly with increasing concentration up to ≈0.2 ppm, but above this level there is relatively little effect on fatigue life from further increases up to 8 ppm. In oxygenated environments, fatigue life depends strongly on strain rate (this dependence on loading history can also be characterized in terms of frequency or rise time) and temperature. For the same environment and the same strain range, lives can vary by a factor of ≈50 depending on the strain rate. At a given strain rate, fatigue life increases by a factor of ≈5 or more as the temperature is decreased from 288° to 200°C.

Empirical Correlations for Effect of Environment on Fatigue Life

Higuchi and Iida[1] correlate their data by assuming that life in the environment is related to life in air at room temperature through a power-law dependence on the strain rate:

$$N_{water} \propto N_{air} (\dot{\varepsilon})^{p} \qquad (1)$$

The strain rate exponent p is a function of temperature (T) and dissolved-oxygen level (O). A best fit to the data is obtained by a piecewise linear relationship of the form

* Work supported by Office of Nuclear Regulatory Research, U.S. Nuclear Regulatory Commission FIN Nos. A22122, and A22562, Program Manager Dr. J. Muscara.

$$p = p_o + M(O)\cdot N(T) \tag{2}$$

where

$$M(O) = \begin{cases} m_l & O \le O_l \\ m_l + (m_h - m_l)\cdot\dfrac{(O - O_l)}{(O_h - O_l)} & O_l < O \le O_h \\ m_h + k_0\cdot(O - O_h) & O_h < O \end{cases} \tag{3}$$

$$N(T) = \begin{cases} k_{100}\cdot\dfrac{T}{100} & T \le 100 \\ k_{100} + (k_{200} - k_{100})\cdot\dfrac{(T-100)}{100} & 100 < T \le 200 \\ k_{200} + (k_{300} - k_{200})\cdot\dfrac{(T-200)}{100} & 200 < T \end{cases} \tag{4}$$

The specific values for the constants p_o, m_l, O_l, ... (for strain rates expressed in $\%\cdot s^{-1}$) chosen by Higuchi and Iida for carbon steel and a low-sulfur (0.003 wt.%) low-alloy steel are given in Table 1.

Table 1. Coefficients in Piecewise Linear Correlation for Strain Rate Exponent p Determined by Higuchi and Iida[1]

	p_o	m_l	O_l	m_h	O_h	k_0	k_{100}	k_{200}	k_{300}
Carbon Steel	0.1	0	0.1	1	0.2	0	0.2	0.2	0.6
Low-Alloy Steel	0.1	0	0.1	1	0.2	0	0.175	0.175	0.25

The tests by Terrell[5] and Hicks and Shack[7] suggest an effect of temperature on fatigue life even in air that is relatively independent of strain rate. This suggests that Eq. 1 take the modified form:

$$N_{water} \propto N_{air}\,\Phi(T)\cdot(\dot{\varepsilon})^p \tag{5}$$

Examination of the Japanese data on fatigue life in air at in the FADAL data base* shows less effect of temperature than was observed by Terrell[5] and Hicks and Shack.[7] At present the reasons for these differences are not clear. The data in Refs. 1–6 and some recent data obtained at Argonne National Laboratory (ANL)** were reanalyzed using Eq. 5 with p in the form given by Eqs. 2–4 and with $\Phi(T)$ in the form

$$\Phi(T) = \alpha e^{\beta/(T+273)} \tag{6}$$

---

*Private communication from M. Higuchi, IHI, to M. Prager of the Pressure Vessel Research Council, January 1992.

**Private communication, Omesh Chopra, ANL, November 1992.

The resulting expression for the strain-rate exponent p for high-sulfur steel differs slightly from that given by Higuchi and Iida.[1] The new coefficients of the piecewise linear expression for p are given in Table 2. In Eq. 6 the coefficients α and β are 0.6 and 148.5, respectively.

Table 2. Revised Coefficients in Piecewise Linear Correlation for Strain Rate Exponent p

	p_o	m_l	O_l	m_h	O_h	k_0	k_{100}	k_{200}	k_{300}
High-sulfur Steel	0.04	0	0.1	1	0.2	0.04	0.26	0.26	0.49
Low-sulfur Steel	0.1	0	0.1	1	0.2	0	0.175	0.175	0.25

The coefficients for low-sulfur steel are identical to those given by Higuchi and Iida[1] for their low-alloy steel. Recent tests at ANL suggest that there is little difference in susceptibility to environmental degradation of fatigue life between low-alloy and carbon steels with comparable sulfur levels. The strong dependence on oxygen level below 0.2 ppm and the relatively weak dependence at higher levels, which are reflected in the values given in Table 2, are consistent with the results of Nagata et al.[8] on low-alloy steels. Figure 1 presents a comparison between the observed lives in the tests of Higuchi and Iida,[1] the data from Dresden,[2] and the tests at B&W[6] and those predicted by Eq. 5, with p determined by the coefficients given in Table 2. In Fig. 1, the mean air curve for carbon steels that was used to develop the current ASME Section III design curve has been used as the reference curve. Better agreement can be obtained if the actual air data for the particular heat of steel are available and are used as the reference curve, as is shown in the case of the Higuchi and Iida data in Fig. 2. Even with the ASME mean air curve, the predicted lives are in reasonably good agreement with the observed lives. It should be noted, however, that virtually all the available experimental data in reactor environments are at relatively high strain ranges, and the validity of Eqs. 1 or 5 at low strain ranges remains to be demonstrated.

Equation 1 or 5 predicts a critical role of the applied strain rate on fatigue life. For water with 0.2 ppm dissolved oxygen and at 288°C (550°F), the strain-rate exponent p is ≈0.5. Typical transients may give strain rates of 0.01–0.001 % s^{-1}. From Eq. 1 or 5 this corresponds to reductions in fatigue life by factors of 10–30. However, some transients may have strain rates of 0.0001–0.00001 % s^{-1}. In these cases, Eq. 1 gives predicted reductions in fatigue life by a factor of >300. The relatively good service experience of carbon steel piping in BWRs suggests that extrapolation of the power-law relation in Eq. 1 or 5 to such low strain rates is unrealistic and that the effect of strain rate on fatigue life must saturate at some level, although no such saturation was observed in the tests of Higuchi and Iida.[1]

Recent tests at ANL on A106-Gr B steel in deionized water with 0.6–0.8 ppm dissolved oxygen at 288°C (550°F) suggest that the decrease in fatigue life does saturate at low strain rates, as shown in Fig. 3. While these results are suggestive, the data currently available at very low strain rates are insufficient to convincingly demonstrate saturation at low strain rates. However, we have tried to develop interim fatigue design curves that are consistent

with the available data, but that use insight gained from fracture mechanics models and engineering judgment to supplement the available data.

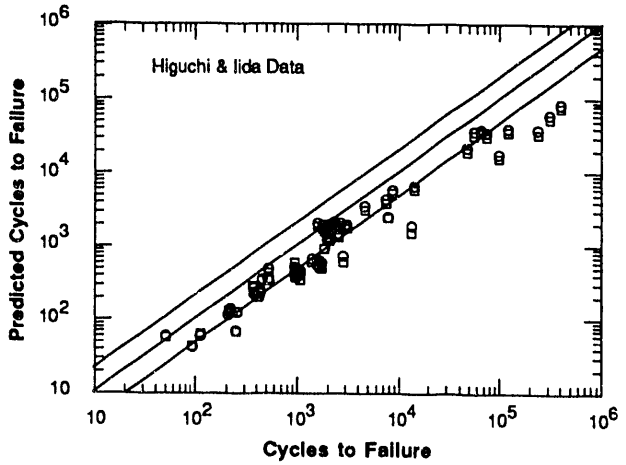

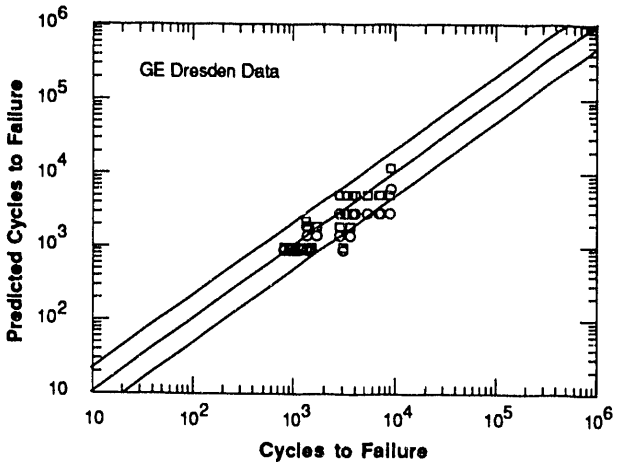

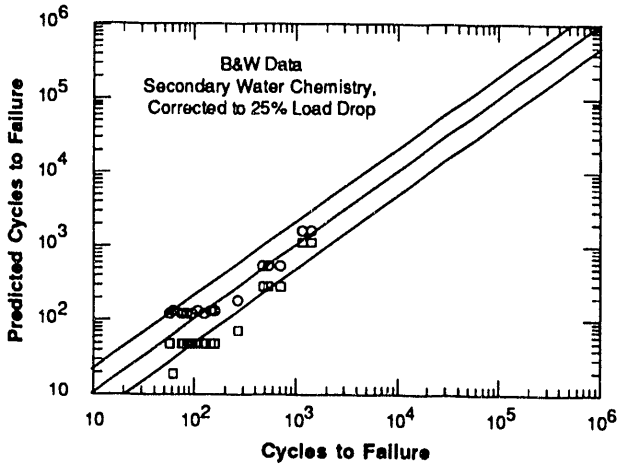

Figure 1.
Comparisons of Predicted Lives with Those Observed in Tests of Higuchi and Iida, GE Tests at Dresden, and Tests at B&W. Air data curve used to develop the ASME Section III design curve is used as the reference curve.

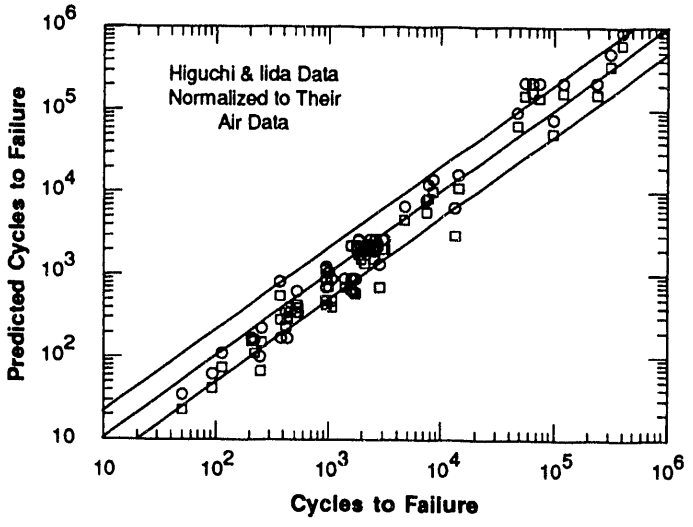

Figure 2.
Comparison of Predicted and Observed Lives in Tests of Higuchi and Iida Using Air Data for Their Heat as the Reference Curve.

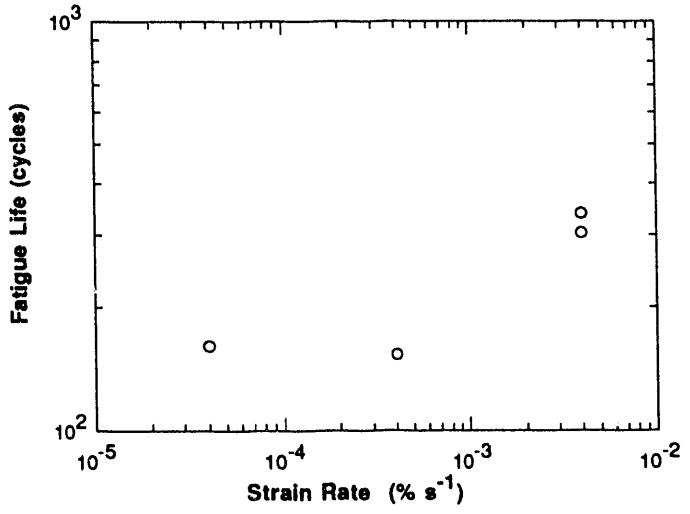

Figure 3.
Fatigue Life in Water with ≈0.8 ppm Dissolved Oxygen at 288°C at a Strain Range of 0.75% as a Function of Strain Rate during Rising Load Portion of Cycle

Development of a Fracture Mechanics Model for Prediction of Fatigue Lives

The life of a "smooth" fatigue specimen has long been recognized to consist of a crack nucleation phase and a crack growth or propagation phase. At low strain ranges (i.e., high-cycle fatigue), life is dominated by the crack nucleation phase, while high strain ranges (i.e., low-cycle fatigue) the crack growth phase dominates. Crack nucleation life is controlled by the strength of the material and is assumed to depend primarily on the applied stress range (or elastic strain range). Crack growth life is controlled by the ductility of the material and depends primarily on the applied plastic strain range. In general, the effect of the environment on crack nucleation life would be expected to be different from that on crack propagation life.

The data of Terrell[5] on SA 106-Gr B steel have been used to estimate the mean fatigue life of carbon steel at 288°C (550°F) in air. This mean curve is shown in Fig. 4a, along with the estimated crack nucleation, N_i, and crack propagation, N_p, life curves based on the assumption that N_i depends on the applied elastic strain range and N_p depends on the applied plastic strain range. Although the curves in Fig. 4a are obtained from the fatigue and cyclic stress/strain data of Terrell,[5] the fatigue curve obtained by Terrell[5] is similar to the mean curve used to generate the current design fatigue curve of the ASME Code, Section III.

N_i is a function of the applied stress range $\Delta\sigma$, although it can also be expressed in terms of the applied strain range through the cyclic stress/strain curve; for SA 106-Gr B at 288°C (550°F) in air, a power-law best fit gives ($\Delta\sigma$ in MPa)

$$\Delta\sigma = 2{,}000 N_i^{-0.0845} \qquad (7a)$$

or

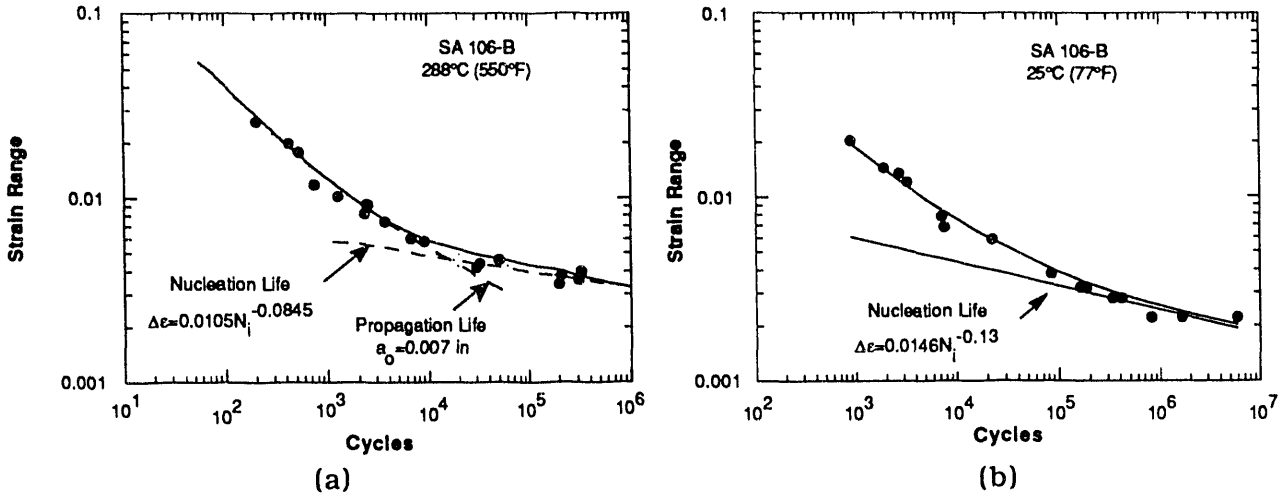

Figure 4. Fatigue Curves for (a) Carbon Steel Tested in Air at 288°C and (b) Room Temperature (25°C)

$$\Delta\varepsilon = 0.0105N_i^{-0.0845} \tag{7b}$$

At room temperature, crack nucleation life is given by (Fig. 4b):

$$\Delta\sigma = 3020N_i^{-0.13} \tag{8a}$$

or

$$\Delta\varepsilon = 0.0146N_i^{-0.13} \tag{8b}$$

The crack propagation life N_p in air at 288°C (550°F) can be expressed in terms of the strain range:

$$\Delta\varepsilon = 0.210N_p^{-0.4055} \tag{9}$$

At room temperature,

$$\Delta\varepsilon = 0.244N_p^{-0.3758} \tag{10}$$

The total life N_f can then be expressed as the sum of the crack nucleation and crack propagation lives

$$N_f = N_i + N_p \tag{11}$$

A fracture mechanics model can be used to calculate the effect of the environment on N_p. Dowling[9] has demonstrated that by characterizing the fracture mechanics crack growth

rate in terms of ΔJ, fracture mechanics analyses can be used to develop estimates of the fatigue life at high strain ranges by computing the number of cycles required for the crack to grow from an initial flaw size a_o to failure. Good agreement is obtained between the lives observed in air with those predicted by Dowling's model when propagation life is computed using the crack-growth-rate curve in air given in the current proposed revision to Section XI of the ASME Code with an initial flaw a_o = 0.002 in. and with failure assumed to occur at a final crack size of 0.1 in. For lower strain ranges, the crack nucleation life N_i can then be interpreted as the number of cycles needed to nucleate a crack of ≈0.002 in. Crack propagation life in the environment can then be obtained by calculating the number of cycles required to grow from a_o to failure using the crack-growth-rate curve for carbon steels in LWR water currently being proposed for inclusion in Section XI.[10]

In Fig. 5, the lives predicted by the fracture mechanics model at a strain range of 1.2% as functions of the strain rate are compared with the data of Higuchi and Iida[1] at this strain range in water with 8 ppm dissolved oxygen at 290°C (554°F). According to the proposed Section XI crack growth curves, at 288°C (550°F) high rates of environmentally assisted cracking (EAC) occur only above a critical threshold value of ΔK, which depends on the rise time.[10] At lower temperatures, this threshold behavior has not been clearly demonstrated.[10] The calculations have been performed by assuming that this threshold behavior occurs (the curve denoted "With Threshold") and that it does not occur (the curve denoted "Without Threshold"). At this strain range, inclusion or neglect of crack nucleation life makes little difference on predicted total life. While the actual values of the predicted lives differ significantly from the observed lives, the dependence on strain rate predicted by the model is similar to the power-law dependence obtained from the empirical relation Eq. 1 down to a strain rate of $\approx 10^{-5} \cdot s^{-1}$. Below that level, the decrease in life with decreasing strain rate is predicted to saturate; the life may even increase in the case where crack growth exhibits an EAC threshold. As noted previously, saturation appears to have been observed in recent tests at ANL; data that demonstrate recovery in fatigue life at very low strain rates have been reported in the Russian literature.[11]

At a strain range of 0.6%, the inclusion or neglect of crack nucleation life has a large influence on predicted total life, as shown in Fig. 6. If no loss in crack nucleation life in water is assumed, the predicted lives become increasingly nonconservative with decreasing strain rate. An analysis that assumes zero crack nucleation life and no threshold in the EAC growth rate predicts lives that are in reasonable agreement with the available experimental data. Saturation is again predicted at strain rates less than $10^{-5} \cdot s^{-1}$. Also, as before, the experimental data appear to be more consistent with the predictions of a crack growth model without an EAC threshold than with a crack growth model with an EAC threshold.

Calculations at other strain ranges show that the predicted value of the saturation strain rate depends only weakly on the applied strain range. For strain rates of 10^{-2} to 10^{-5} s^{-1}, the variation of relative life with strain rate predicted by the fracture mechanics model is similar to the power-law behavior used to fit the data from conventional fatigue tests. For strain ranges of 0.3–1.2%, the strain-rate exponents obtained from the fracture mechanics model range from 0.5 to 0.6, compared to 0.50 obtained from the parameters given in Table 2.

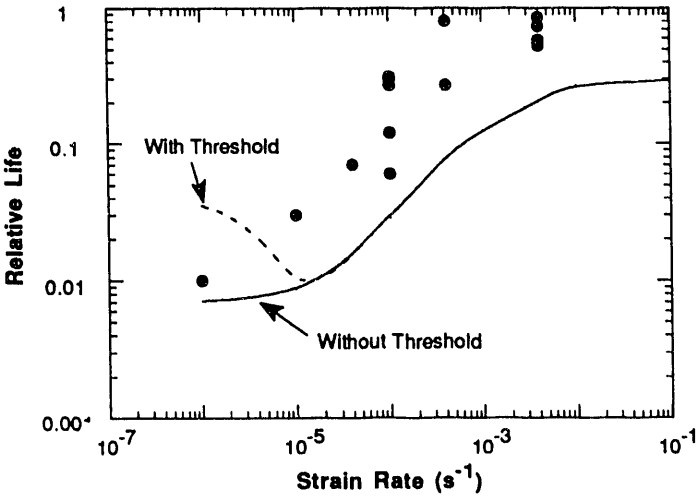

Figure 5.
Comparison of Predicted and Observed Fatigue Lives of a Carbon Steel as Functions of Strain Rate for Tests Conducted at Strain Range of 1.2% in 288°C (550°F) Water Containing 8 ppm Dissolved Oxygen.

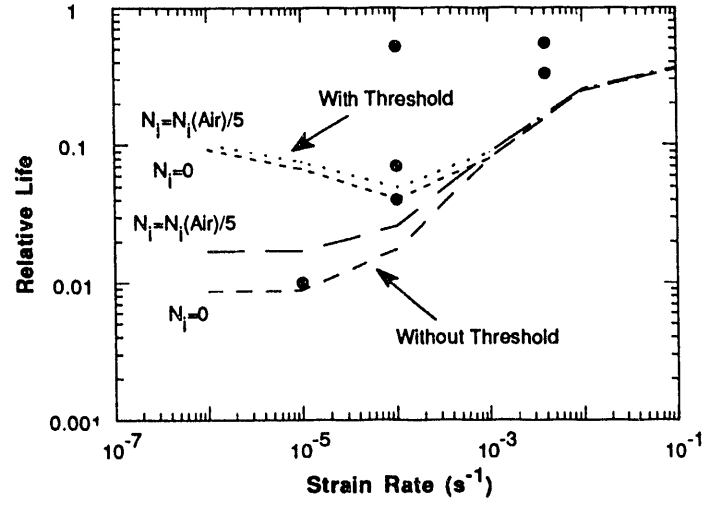

Figure 6
Comparison of Predicted and Observed Fatigue Lives of a Carbon Steel as Functions of Strain Rate for Tests Conducted at Strain Range of 0.6% in 288°C (550°F) Water Containing 8 ppm Dissolved Oxygen.

Proposed Interim EAC–Adjusted Fatigue Curve for Carbon Steels

The critical conclusion from the fracture mechanics modeling studies is the existence of a saturation strain below which fatigue life does not decrease with decreasing strain rate (indeed, it is possible that there is recovery in life at strain rates below this critical value). The model predicts that this critical strain rate is $\approx 10^{-5}$ s^{-1}. This value is consistent with the preliminary experimental results shown in Fig. 3. Although N_p can be estimated from the model, the interim curves are based on data from conventional fatigue tests, and the fracture mechanics results are invoked only to justify the introduction of saturation at low strain rates.

Both crack propagation life, N_p, and crack nucleation life, N_i, depend on the critical environmental variables of dissolved-oxygen concentration and temperature and on the applied strain rate. The model of Higuchi and Iida[1] assumes that N_p and N_i show the same dependence on the environmental variables and strain rate. However, most of their tests are at such high strain range values that crack nucleation life is negligible and only the variation in N_p is well defined by their data. We assume that N_p is of the form given by Eq. 5

$$N_{p_{water}} \propto N_{p_{air}} \Phi(T)\, \dot{\varepsilon}^{p} \qquad \dot{\varepsilon} \geq 10^{-5}\ s^{-1} \qquad (12)$$

where the strain-rate exponent p is a function of oxygen and temperature, as given by Eqs. 2 and 3 and Table 2, and the effect of the strain rate is assumed to saturate at a strain rate of 10^{-5}·s^{-1}. There appears to be a sharp threshold in fatigue life at dissolved-oxygen levels between 0.1 and 0.2 ppm.[1] Because of the large uncertainties in life for oxygen levels in the threshold region, we conservatively take the threshold level at the lower 0.1 ppm level.

Because fewer data are available for N_i, more reliance must be placed on engineering judgment. Terrell[5] has noted that carbon steels such as SA-106 Gr B exhibit strain aging at reactor operating temperatures. Tensile tests at various temperatures conducted recently at Battelle-Columbus[12] on SA-333 Gr 6 and SA-106 Gr B specimens obtained from pipes of various diameters have shown that the magnitude of the increase in ultimate tensile strength (UTS) due to strain aging can vary significantly (the observed increases range from 1.09 to 1.30 relative to the UTS at room temperature) from pipe to pipe even for the same heat of material. Because the high-cycle fatigue life depends on the strength of the material, it will increase if strain aging occurs, and in this case N_i could increase with decreasing strain rate.[13] Terrell's data[5] show that the stress-versus-fatigue-life curves (at $4 \cdot 10^{-3}$ s^{-1}) at room temperature and at 288°C (550°F) cross over in the high-cycle fatigue regime. However, degradation of high-cycle fatigue life can occur through a variety of environmentally induced processes such as the formation of surface pits, which cause stress concentrations and consequently reduce high-cycle fatigue life. Even without macroscopic pitting, micropitting occurs at the sites of MnS particles in high-sulfur carbon and low-alloy steels in oxygenated water. Examination of the specimens tested at ANL in 288°C (550°F) oxygenated water shows that the cracks in the specimens virtually always initiate at such pits. Of course, the film rupture and dissolution processes usually associated with crack propagation[14] could also affect nucleation life.

The net effect of these competing mechanisms may vary from heat to heat and will be dependent on material composition, dissolved-oxygen level, temperature, and exposure history. For stainless steels, corrosion processes appear to increase the life at strain ranges below 0.25% over that observed in air.[15] For ferritic steels, the data currently available are inadequate to accurately characterize crack nucleation life. Two different assumptions have been examined. In one, N_i is assumed to degrade due to micropitting in oxygenated water, which results in a net effective stress concentration factor (K_f) of 1.2 and a consequent reduction in life by a factor of ≈5. In the other, the approach of Higuchi and Iida[1] is followed and N_i is assumed to have the same dependence on strain rate as N_p. As in the case of propagation life, the effect of strain rate is assumed to saturate at 10^{-5} s^{-1}. The limited data available at relatively low strain ranges[1,5] seem to be in better agreement with the Higuchi and Iida assumption, which also gives more conservative predictions. The threshold strain range for environmental effects is estimated to be 0.2%, based on the data in Ref. 4. The basis for a threshold could be either a critical strain for oxide film rupture[14] or improvement in high-cycle fatigue life due to strain aging. The 0.2% limit is expected to be a conservative estimate of this threshold value, but additional data are needed before better estimates can be made. Thus

$$N_{p_{water}} \propto N_{p_{air}} \Phi(T)\, \dot{\varepsilon}^{p},\ N_{i_{water}} \propto N_{i_{air}} \Phi(T)\, \dot{\varepsilon}^{p} \qquad \dot{\varepsilon} \geq 10^{-5}\ s^{-1} \qquad \Delta\varepsilon > 0.2\% \qquad (13)$$

The estimates of $N_{f_{air}}$ and $N_{p_{air}}$ are based on the mean curve used to generate the current design fatigue curve of the ASME Code, Section III. In terms of the applied strain range,

$$\Delta\varepsilon = 0.012\, N_f^{-0.13} \tag{14a}$$

$$\Delta\varepsilon = 0.51 N_p^{-0.469} \tag{14b}$$

The resulting fatigue life curves are shown in Fig. 7 for T = 200, 250, and 288°C for strain rates corresponding to saturation ($\leq 10^{-5}$ s^{-1}), 0.0001, and 0.001 s^{-1}. The curves at saturation will be good estimates of the fatigue life at low strain rates and conservative estimates of the fatigue life at higher strain rates. The reduction in fatigue life at this saturation value is strongly dependent on dissolved-oxygen level and temperature. Because these curves describe the mean life of small laboratory specimens, the standard ASME factors of "2 on stress or 20 on cycles" must be applied to obtain the corresponding design curves for components, as shown in Fig. 8.

For water with ≤0.1 ppm dissolved oxygen at ≤320°C, environmental degradation is

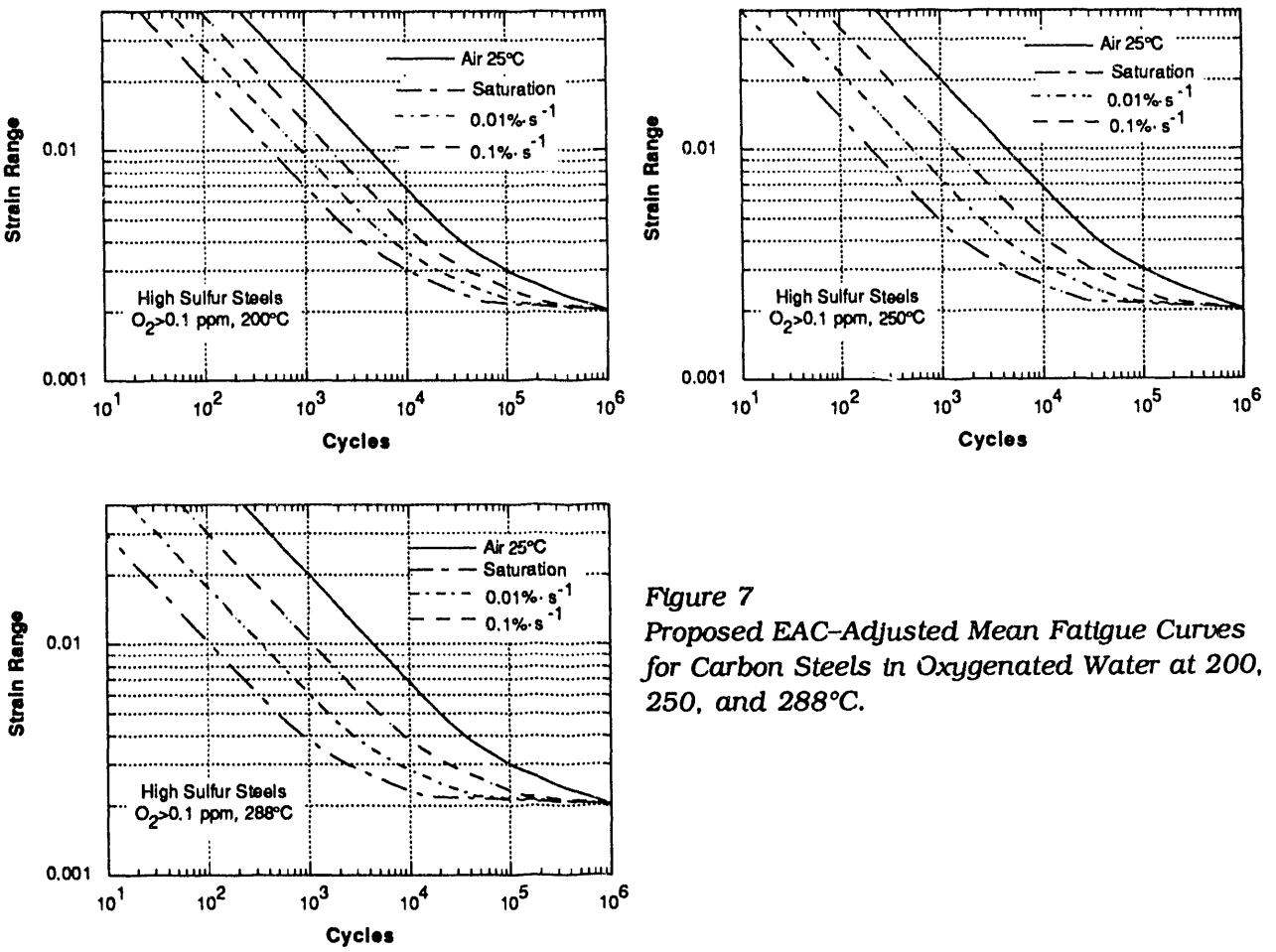

Figure 7
Proposed EAC-Adjusted Mean Fatigue Curves for Carbon Steels in Oxygenated Water at 200, 250, and 288°C.

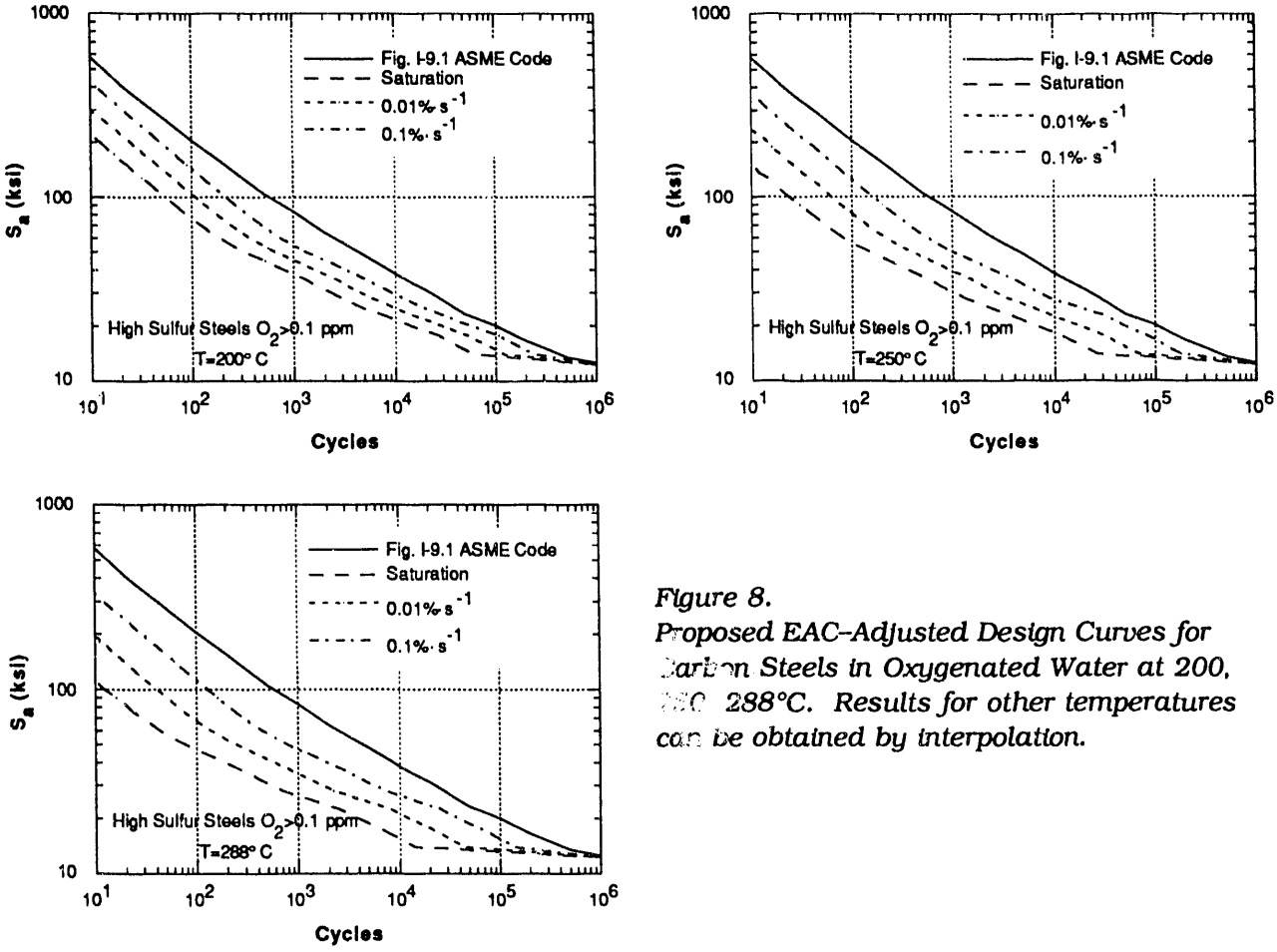

Figure 8.
Proposed EAC-Adjusted Design Curves for Carbon Steels in Oxygenated Water at 200, 250, 288°C. Results for other temperatures can be obtained by interpolation.

greatly reduced and an estimate of the mean-fatigue-life curve at saturation is given by

$$N_{p_{water}} = \frac{N_{p_{RT}}}{2} \qquad N_{i_{water}} = \frac{N_{i_{RT}}}{2}. \tag{15}$$

A threshold strain range of 0.2% for any environmental effect is still assumed. The resulting fatigue-life curve is shown in Fig. 9. Because this curve again describes the mean life of small laboratory specimens, the standard ASME factors of "2 on stress or 20 on cycles" must be applied to obtain the corresponding design curve for components as shown in Fig. 10.

The proposed interim design curves for oxygenated water are thought to be consistent with the screening criteria proposed in the draft USNRC Branch Technical Position (BTP) on Fatigue for BWRs,* assuming that the BTP criteria given for BWRs applies to systems with dissolved-oxygen levels greater than 0.1 ppm. The degree of conservatism in the BTP screening criterion will depend on the actual cyclic histories. Compared to the proposed interim curves, the screening criterion is nonconservative for low strain rates, but is more conservative than the interim curves for higher strain rates. We believe that in most cases

*USNRC Branch Technical Position PDLR D-1, Fatigue Evaluation Procedures, Draft, December 1991.

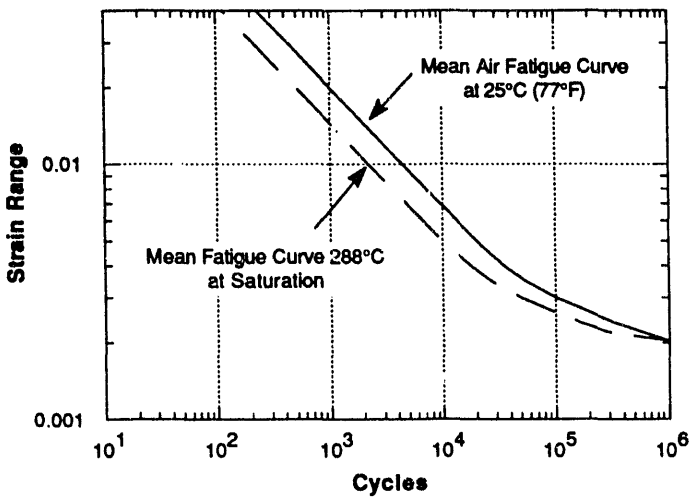

Figure 9.
Proposed EAC-Adjusted Mean Fatigue Curve for Carbon Steels in Water with ≤0.1 ppm Dissolved Oxygen.

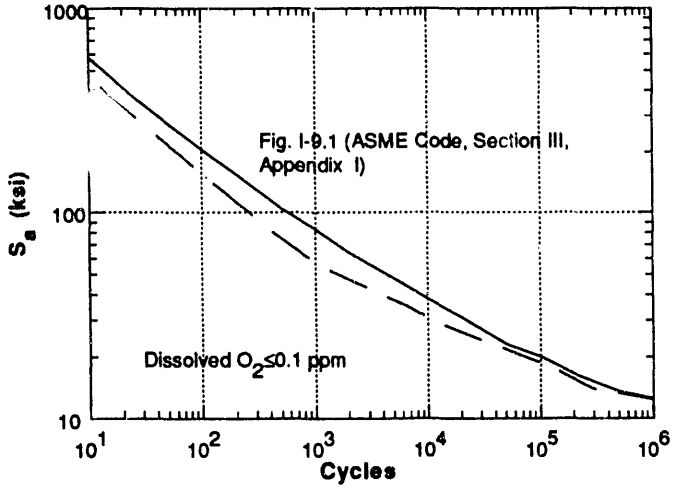

Figure 10.
Proposed EAC-Adjusted Design Curve for Carbon and Low-Alloy Steels in Water with ≤0.1 ppm Dissolved Oxygen

it will give adequately conservative assessments. The proposed interim design curve for low-oxygen water is, as expected, somewhat less conservative than the corresponding screening criterion in the BTP. In this case, the proposed screening factor bounds the curve for all strain ranges.

Proposed Interim EAC-Adjusted Fatigue Curves for Low-Alloy Steels

Low-alloy steels also show a decrease in fatigue life in oxygenated water.[1,8] The magnitude of the decrease is again dependent on the strain rate, but the strain rate exponents determined from the data reported in Refs. 1 and 8 are typically smaller than those for carbon steels, as determined from Eqs. 2-4 and the values in Table 1. However, the sulfur contents in the alloys studied by the Japanese are low (0.003 and 0.008 wt.%) compared to those found in current US reactors. Nagata et al.[8] compared two materials, an SA 508 forging with 0.003 wt.% S, and an SA 533-Gr B plate with 0.008 wt.% S. The higher-sulfur material showed more degradation in fatigue life in oxygenated water. Initial tests on a high-sulfur low-alloy steel at ANL suggest that degradation in life in oxygenated water is comparable to that observed in a high-sulfur carbon steel. Thus, at least tentatively, it

seems reasonable to assume that it is primarily the sulfur content that determines the susceptibility of either carbon or low-alloy steels to degradation of fatigue life.

Fatigue crack growth studies have demonstrated[16] that it is somewhat naive to classify materials as "low-sulfur" and "high-sulfur" on the basis of bulk sulfur content alone. However, we will tentatively assume that low-alloy steels with sulfur levels >0.008 wt.% will behave like the carbon steels and that materials with sulfur levels below this will show less susceptibility to loss of fatigue life. In low-oxygen water (≤0.1 ppm), loss in fatigue life is small even for materials with high sulfur levels.[7]

For low-alloy steels with <0.008 wt.% S, the interim curves are based on the work of Higuchi and Iida.[1] Their work suggests that the strain-rate exponent for these steels is ≈0.3 in environments with >0.1 ppm dissolved oxygen. We again assume that the strain rate effect saturates at 10^{-5} s^{-1} (0.001% s^{-1}). The effect of temperature is smaller than for the carbon steels, and a reduction factor of 10 at saturation can be used for temperatures between 200–300°C. The resulting design curve for low-sulfur steels is shown in Fig. 11.

Proposed Interim EAC–Adjusted Fatigue Curves for Austenitic Stainless Steels

Austenitic stainless steels also show degradation in fatigue life in oxygenated water.[15] The magnitude of the decrease is again dependent on strain rate, but the strain-rate exponent is typically lower (≈0.18) than in carbon or low-alloy steels. No data are available on the variation with temperature or the effect of low dissolved oxygen, although presumably the data in Ref. 15 in water with 0.2 ppm dissolved oxygen at 288°C (550°F) bounds the degradation expected at lower levels of dissolved oxygen and lower temperatures.

Fracture mechanics analyses using the crack growth curves for austenitic stainless steels in Ref. 17 give results consistent with conventional fatigue tests. However, no saturation or recovery in fatigue life is observed at very low strain rates as is the case for carbon steels. More mechanistic studies of crack growth suggest that there is a threshold velocity below which environmentally assisted crack growth will cease.[14] For example, crack blunting will occur when corrosion rates at the crack tips become comparable to those on

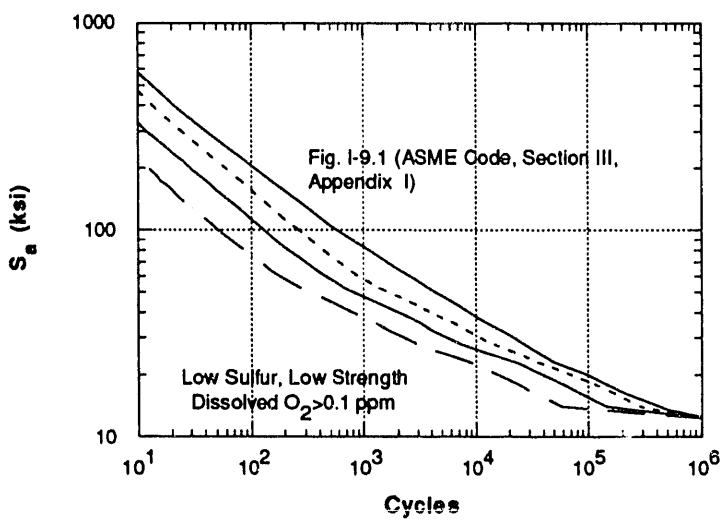

Figure 11.
Proposed EAC-Adjusted Design Curves for Low-Sulfur Steels in Water with >0.1 ppm Dissolved Oxygen

the crack flanks. In austenitic stainless steels, such threshold velocities are very low and difficult to measure directly. However, a saturation strain rate of 10^{-5} s^{-1} corresponds to a threshold velocity of $\approx 5 \cdot 10^{-13}$ $m \cdot s^{-1}$, which is consistent in magnitude with the values conjectured in mechanistic studies.[14] This value for the strain rate at saturation and the measured value of the strain rate exponent $p \approx 0.18$, (Ref. 15) suggest that the maximum estimated reduction in propagation life corresponds to a reduction factor of 4.

The data in Ref. 15 suggest that N_i in water with 0.2 ppm dissolved oxygen at 288°C (550°F) is comparable to that observed in air at room temperature. Thus an estimate for mean-fatigue life in the environment at the saturation strain rate is given by

$$N = \frac{N_{p_{RT}}}{4} + N_{i_{RT}} \tag{16}$$

The corresponding life as a function of strain range is shown in Fig. 12. Again, because most of the experimental data are obtained at strain rates $>10^{-5}$ s^{-1}, the experimental data from Ref. 15 lie above the curve in most cases.

A design curve can be obtained from this mean curve by adding appropriate safety factors. The original ASME Design Curve for austenitic stainless steels was based on tests in air at room temperature and at relatively high strain ranges. The design curve was then obtained by applying the standard factors of "2 on stress or 20 on cycles." In the early 1970s, additional data on the fatigue of stainless steels were collected by Jaske and O'Donnell, and a revised room-temperature fatigue curve was developed.[18] Comparison of the new curve developed by Jaske and O'Donnell showed that the original curve overestimated life for low strain ranges. However, the ASME Code Committee, because of relatively good in-plant experience, did not lower the corresponding portion of the design curve. In

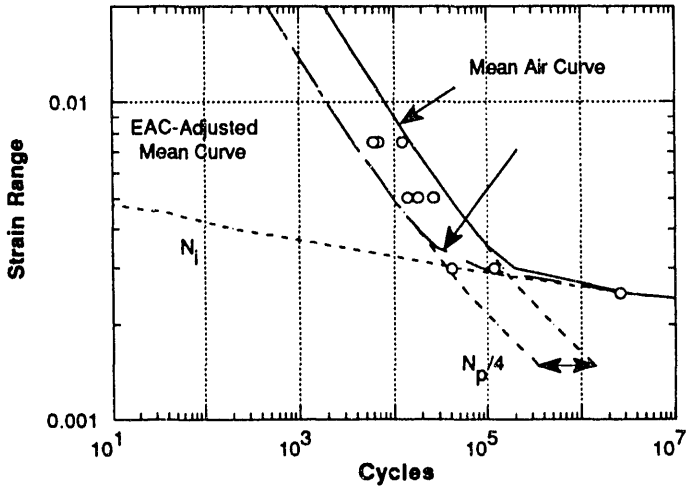

Figure 12.
Proposed EAC-Adjusted Mean-Fatigue Curve for Austenitic Stainless Steels in Water at 288°C with Data from Ref. 15.

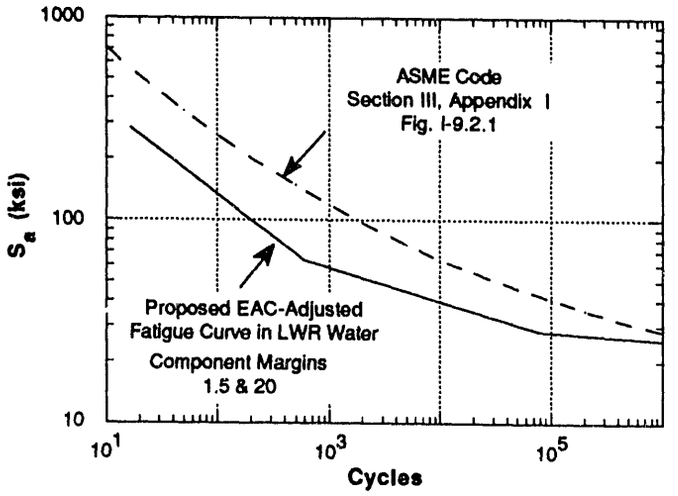

Figure 13.
Proposed EAC-Adjusted Design Curves for Austenitic Stainless Steels in Water at Temperatures between 200 and 320°C.

effect, the current curve is based on a factor of 1.5 on stress and 20 on cycles rather than the "2 on stress or 20 on cycles" originally proposed.*

The design curve shown in Fig. 13 uses a factor of 1.5 on stress and 20 on cycles. The mean curve and the design curve are based on data obtained in water with 0.2 ppm dissolved oxygen. Because data on fatigue of stainless steels at low strain rates in water with low dissolved oxygen are very sparse, the present interim design curve is recommended for use at all oxygen levels until additional data become available.

References

1. M. Higuchi and K. Iida, Fatigue Strength Correction Factors for Carbon and Low-Alloy Steels in Oxygen-Containing High-Temperature Water, *Nuclear Engineering and Design*, **129**, pp 293–306 (1991).

2. D. A. Hale, S. A. Wilson, E. Kiss, and A. J. Gianuzzi, *Low Cycle Fatigue Evaluation of Primary Piping Materials in a BWR Environment*, GEAP-20244, U.S. Nuclear Regulatory Commission (September 1977).

3. D. A. Hale, S. A. Wilson, J. N. Kass, and E. Kiss, Low Cycle Fatigue Behavior of Commercial Piping Materials in a BWR Environment, *J. of Eng. Mat. and Tech.* **103**, pp 15–25 (1981).

4. S. Ranganath, J. N. Kass, and J. D. Heald, Fatigue Behavior of Carbon Steel Components in High-Temperature Water Environments, *Low-Cycle Fatigue and Life Prediction*, ASTM STP 770, C. Amzallag, B. N. Leis, and P. Rabbe, eds., American Society for Testing and Materials, pp. 436–459 (1982).

5. J. Terrell, Effect of Cyclic Frequency on the Fatigue Life of ASME SA-106-B Piping Steel in PWR Environments, *J. Mater. Eng.*, **10**, pp 193–203 (1988).

*Private communication, Carl Jaske, CorTest Technology, to Saurin Majumdar, ANL, July 1992.

6. B. A. James, L. D. Paul, and M. T. Mighlin, "Low Cycle Fatigue Crack Initiation in SA-210 A1 Carbon Steel Boiler Tubing in Contaminated Boiler Water," *Fatigue, Degradation and Fracture, PVP-Vol. 195*, W. H. Bamford, C. Becht, S. B. Framatome, J. D. Gilman, L. A. James, and M. Prager, eds., American Society of Mechanical Engineers, pp 13–19 (1990).

7. P. D. Hicks and W. J. Shack, "Fatigue of Ferritic Steels," Environmentally Assisted Cracking in Light Water Reactors Semiannual Report April–September 1991, NUREG/CR-4667, ANL-92/6, Vol. 13, pp 3–8 (March 1992).

8. N. Nagata, S. Sato, and Y. Katada, Low Cycle Fatigue Behavior of Low Alloy Steels in High Temperature Pressurized Water, *Transactions of the 10th International Conf. on Structural Mechanics in Reactor Technology, Volume F*, A. H. Hadjian, ed., American Association for Structural Mechanics in Reactor Technology, Anaheim, CA (1989).

9. N. E. Dowling, Crack Growth During Low-Cycle Fatigue of Smooth Axial Specimens, *Cyclic Stress-Strain and Plastic Deformation Aspects of Fatigue Crack Growth*, ASTM STP 637, American Society for Testing and Material, Philadelphia, PA, pp. 97–121 (1977).

10. E. D. Eason, "EDEAC Status; Analysis Porcedures for da/dN and S–N Data," Technical Information from Workshop Cyclic Life and Environmental Effects in Nuclear Applications, Vol. 2, Clearwater Beach, FL, Pressure Vessel Research Committee and Welding Research Council (January 20–21, 1992).

11. V. M Filatov, A. I. Gromova, V. G. Denisov, and V. G. Vasil'ev, Corrosion Fatigue Test of Steel in Coolant Water, *Ind. Lab.* (USSR) **48**, pp 385–388 (1982). Translated from *Zavodskaya Laboratoriya*, **48**, pp 64–67 (1982).

12. G. M. Wilkowski, F. Brust, R. Francini, N. Ghadiali, T. Kilinski, P. Krishnaswamy, M. Landow, C.W. Marshall, S. Rahaman, and P. Scott, *Short Cracks in Piping and Piping Welds*, Semiannual Report Oct. 1990– Mar. 1991, NUREG/CR-4599, BMI-2173, Vol.1, No. 2 (1992).

13. H. Abdel-Raouf, A. Plumtree, and T. H. Topper, "Effects of Temperature and Deformation Rate on Cyclic Strength and Fracture of Low-Carbon Steel," *Cyclic Stress-Strain Behavior—Analysis, Experimentation, and Failure Prediction*, ASTM STP 519, L.F. Coffin and Erhard Krempl, symposium co-chairmen, American Society for Testing and Materials, pp. 28–57 (1973).

14. F. P. Ford, D. F. Taylor, P. L. Andresen, and R. G. Ballinger, *Corrosion-Assisted Cracking of Stainless and Low-Alloy Steels in LWR Environments*, EPRI NP-5064S, Electric Power Research Institute, Palo Alto, CA (February 1987).

15. W. J. Shack and W. F. Burke, "Fatigue Life of Type 316NG SS," Environmentally Assisted Cracking in Light Water Reactors Semiannual Report October 1989–March 1990, NUREG/CR-4667, ANL-91/5, Vol. 10, pp 2–6 (March 1991).

16. D. Worswick, D. R. Tice, P. M. Scott, and J. D. Wilson, "Influence of Environmental Variables on Corrosion Fatigue Crack Growth in PWR Pressure Vessel Steels," Proc. 3rd

International Atomic Energy Agency Specialists' Meeting on Subcritical Crack Growth," NUREG/CP-0112, ANL-90/22 Vol. 1 (August 1990).

17. W. J. Shack, "Corrosion Fatigue Curves for Austenitic SS in LWR Environments," Environmentally Assisted Cracking in Light Water Reactors Semiannual Report October 1990–March 1991, NUREG/CR-4667, ANL-91/24, Vol. 12, pp 30–37 (August 1991).

18. C. E. Jaske and W. J. O'Donnell, "Fatigue Design Procedure for Pressure Vessel Alloys," *Trans. ASME J. of Pressure Vessel Technology*, **99** (4), pp 584–592 (November 1977).

END

DATE
FILMED
5/26/93